



# Second and third-order dispersion compensating mirror pairs for the spectral range from 1.2-3.2 $\mu\text{m}$

DANIEL HAHNER,<sup>1,\*</sup>  PHILIPP STEINLEITNER,<sup>2</sup> YU CHEN,<sup>1</sup> KA FAI MAK,<sup>2</sup> AND VLADIMIR PERVAK<sup>1</sup>

<sup>1</sup>*Department of Physics, Ludwig-Maximilians-Universität Munich, Am Coulombwall 1, D-85748 Garching, Germany*

<sup>2</sup>*Max Planck Institute of Quantum Optics, Hans-Kopfermann-Str. 1, D-85748 Garching, Germany*

\**Daniel.Hahner@physik.uni-muenchen.de*

**Abstract:** We demonstrate the design, production, characterization and application of two dispersive complementary mirror pairs compensating second- and third-order dispersion, respectively. Both mirror pairs operate in the spectral range from 1.2-3.2 $\mu\text{m}$ . This is an unprecedented bandwidth of over 1.4 octaves which can drive further improvements in Cr:ZnS, Cr:ZnSe and other laser systems with a central wavelength around 2 $\mu\text{m}$ . The first pair provides a constant group delay dispersion of  $-100\text{fs}^2$ , while the second one enables the compensation of the third-order dispersion that is introduced by a TiO<sub>2</sub> crystal.

© 2022 Optica Publishing Group under the terms of the [Optica Open Access Publishing Agreement](#)

## 1. Introduction

Dispersive mirrors (DM), also known as chirped mirrors, are one of the most important tools in laser systems generating ultrashort pulses and have been continuously improved for nearly three decades at this point [1–6]. Usually the DM development follows the improvements in laser systems closely to meet the laser scientists' demands. While DMs operating in the UV-NIR range are well known and commercially available, there have been several new developments for the mid-infrared (MIR) spectral range recently [7–9]. Especially lasers with a central wavelength around 2 $\mu\text{m}$  like Cr:ZnS, Cr:ZnSe, thulium and holmium based systems gained a lot of interest lately [10–12]. The output of those lasers can be used, for example, as a seed in an OPCPA system [13] or to drive a non-linear process in a GaSe [14] or a ZnGeP<sub>2</sub> [15] crystal. These approaches can generate MIR pulses in the range from 2-20 $\mu\text{m}$ . This is an interesting spectrum for biomedical applications [16] which explains the high demand for improved laser systems driving the generation of broad MIR spectra. With these prerequisites the authors reported a complementary mirror pair in the range from 2-4 $\mu\text{m}$  in [7]. These mirrors provided an overall reflectance exceeding 99.7% and a group delay dispersion (GDD) of  $-200\text{fs}^2$ . At the time, this one octave spanning mirror pair was the best reported achievement so far. By carefully improving coating parameters and after consultation with the laser scientists in our group two different DM pairs were produced for the present work. Since the laser systems shifted towards shorter wavelengths, the DMs were designed to cover a spectrum from 1.2-3.2 $\mu\text{m}$ . Although a notable amount of the spectrum at longer wavelengths has been cut off, the addition of the shorter wavelengths significantly increased the covered bandwidth to over 1.4 octaves compared to the one octave in [7]. All four mirrors are comprised of the same layer materials, namely Si and SiO<sub>2</sub>. Especially the successful production of a complementary pair compensating the third-order dispersion (TOD) introduced by a 0.5mm thick TiO<sub>2</sub> crystal is a big step in the development of infrared dispersive optics and will enable further improvements in 2 $\mu\text{m}$  based laser systems.

In section 2, the design process is explained, the theoretical properties of the mirrors are presented and the production of the four mirrors is described. In section 3, measurements of the

optical properties are shown and the application in a Cr:ZnS laser system is presented. In section 4 a conclusion is drawn.

## 2. Design and production

For the complete design process the OptiLayer software package [17] was used. The specified target for the reflectance over the complete working range of 1.2-3.2 $\mu\text{m}$  was set to 100% for both DM pairs. For the second-order dispersion compensating mirrors the target GDD was defined at  $-100\text{fs}^2$ . This is only half of the amount of GDD compared to [7], but this decrease was necessary to keep the reflectance as high as possible. Nevertheless, the layer number more than doubled to meet the target requirements for the new GDD compensating pair. For the TOD compensating mirrors the target was extracted from a GDD measurement of a 0.5mm thick TiO<sub>2</sub> crystal. This measured GDD roughly corresponds to a constant TOD of  $-300\text{fs}^3$ . Additionally, the two layer materials must be known precisely. The Cauchy formula was used to describe the refractive index  $n$  of Si and SiO<sub>2</sub>:

$$n(\lambda) = A_0 + \frac{A_1}{\lambda^2} + \frac{A_2}{\lambda^4} \quad (1)$$

where  $A_0$  is a dimensionless parameter,  $A_1$  is given in units of  $\mu\text{m}^2$  and  $A_2$  in units of  $\mu\text{m}^4$ . For Si  $A_0 = 3.239220$ ,  $A_1 = 0.091475\mu\text{m}^2$ ,  $A_2 = 0.121507\mu\text{m}^4$  and for SiO<sub>2</sub>  $A_0 = 1.465294$ ,

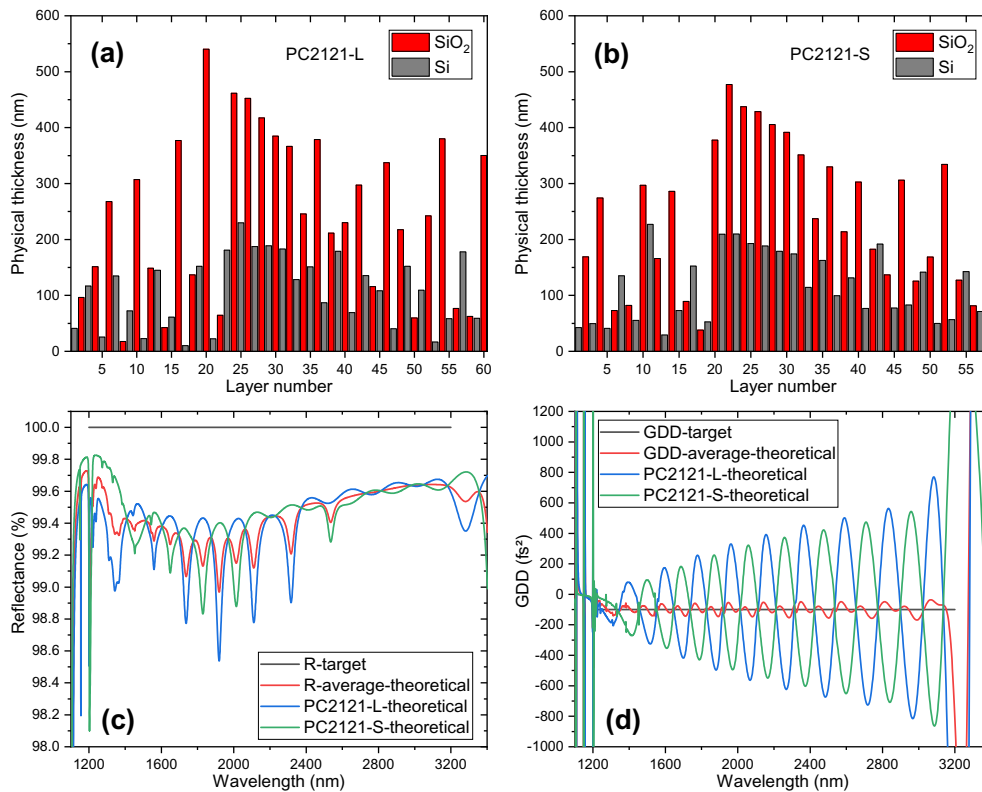


**Fig. 1.** (a) Layer structure of PC2121-L. (b) Layer structure of PC2121-S. (c) Reflectance target, average reflectance upon one bounce and individual reflectance curves of PC2121-L and PC2121-S. (d) GDD target, average GDD per bounce as well as individual GDD of PC2121-L and PC2121-S.

$A_1 = 0.0\mu\text{m}^2$ ,  $A_2 = 0.000471\mu\text{m}^4$ . Due to a working range at shorter wavelengths compared to the authors previous work [7], absorption had to be taken into account for Si for both mirror pairs. Therefore, the extinction coefficient was specified by the Sellmeier formula:

$$k(\lambda) = \left[ n(\lambda) * \left( B_1\lambda + \frac{B_2}{\lambda} + \frac{B_3}{\lambda^3} \right) \right] \quad (2)$$

where  $n(\lambda)$  is specified in Eq. (1),  $B_1 = 703.546\mu\text{m}^{-1}$ ,  $B_2 = 495.765\mu\text{m}$  and  $B_3 = -1627.896\mu\text{m}^3$ .

With the help of the included algorithms in the OptiLayer software and the needle optimization technique [18] the two mirror pair designs could be synthesized. The names for the individual mirrors of the GDD pair are PC2121-L and PC2121-S. For the TOD pair they are TOD2121-L and TOD2121-S. The layer structure for both mirrors of each pair, as well as the theoretical reflectance and GDD curves are presented in Fig. 1 and 2, respectively. The only slight variations of the combined GDDs from the target GDDs, due to the in anti-phase matched GDD oscillations, compared to a single mirror can be clearly observed. In order to keep the GDD performance of the TOD pair within an acceptable range some reflectance had to be sacrificed compared to the GDD mirrors, where the theoretical reflectance for the pair is still above 99% after reflection from both mirrors. Overall 60 and 58 layers were used for PC2121-L/S and 46 layers for both TOD2121-L/S. The specified angle of incidence for all mirrors is  $5^\circ$ .

The designed DM pairs were coated in a Helios magnetron sputtering plant by Bühler Leybold Optics (Alzenau, Germany). Although a broadband monitoring system is available for this

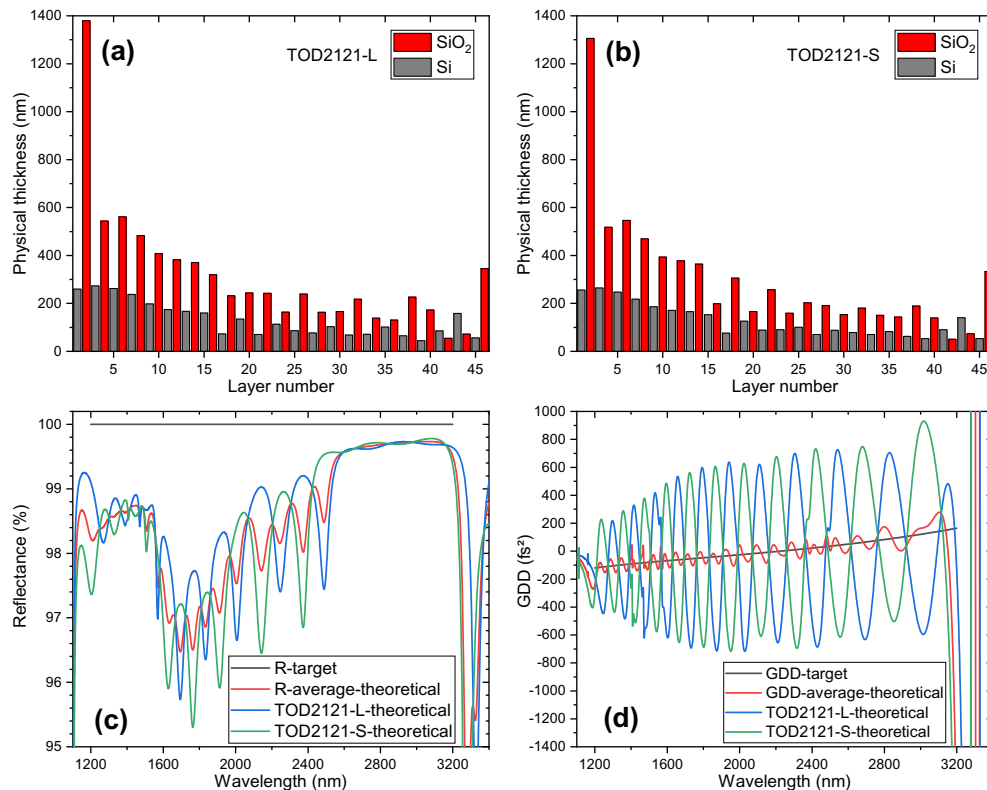


**Fig. 2.** (a) Layer structure of TOD2121-L. (b) Layer structure of TOD2121-S. (c) Reflectance target, average reflectance upon one bounce and individual reflectance curves of TOD2121-L and TOD2121-S. (d) GDD target, average GDD per bounce as well as individual GDD of TOD2121-L and TOD2121-S.

deposition plant, the coating process was controlled using time-control with highly stable sputtering rates. The machine is equipped with two dual-magnetrons and a plasma source for ion-assisted reactive middle frequency dual-magnetron sputtering. The process was tuned towards fast sputtering rates and a high optical layer quality. High quality Suprasil quartz glass was used as the substrate. Argon was used as the sputtering gas. For the SiO<sub>2</sub> layers oxygen was introduced near the Si target to oxidize the sputtered thin films. Before the coating process, the system was pumped down to  $1 \times 10^{-6}$  mbar by several turbo-molecular pumps. During the coating process the pressure was kept at  $1 \times 10^{-3}$  mbar. The power of the cathodes was 4500W. All four mirror designs have a total physical thickness around 10 $\mu$ m and the sputtering rate for Si and SiO<sub>2</sub> is 0.5nm/s for both materials. Therefore, just the coating time was between seven and eight hours for a single mirror. However, this does not include the pumping times, loading and unloading as well as all the other necessary steps to prepare the process. Nevertheless, due to the exceptionally stable coating process the four different mirror types were produced successfully in four subsequent deposition runs.

### 3. Characterization and application

After the deposition, the optical properties of all four mirrors (PC2121-L, PC2121-S, TOD2121-L and TOD2121-S) were measured. The reflectance was measured with a Lambda 950 photospectrometer with the optional Universal Reflectance Accessory (URA) by Perkin Elmer (Waltham, USA) in the range from 1100 to 2650nm. Additionally, to measure the complete working range of the mirrors beyond 2650nm, a commercially available Vertex 70 FTIR spectrometer by Bruker (Billerica, USA) was used. The measurements from both devices were combined and are presented as one curve for each mirror together with the measurement of an unprotected gold mirror for reference in Fig. 3. For the GDD mirrors in Fig. 3(a) the expected features can clearly be seen if theory and measurement are compared for the range from 1600 to 2600nm. For the longer wavelengths a significant drop in reflectance can be observed which is not predicted by the theory. This decrease can be attributed to the well known absorption due to bound hydroxyl [19]. For the shorter wavelengths on the other hand the estimated absorption in Si is not sufficient. This can be avoided in future coatings by recalibrating the optical properties of Si. Overall, the mirrors exceed the reflectance of a gold mirror for most of the spectral range while also providing additional dispersion control. For the TOD pair very similar results can be seen in Fig. 3(b). The mirrors follow the theoretical curves closely as well in the center of the spectral range, while dropping below for the shortest and longest wavelengths for the same reasons as the GDD pair (stronger absorption and bound hydroxyl).

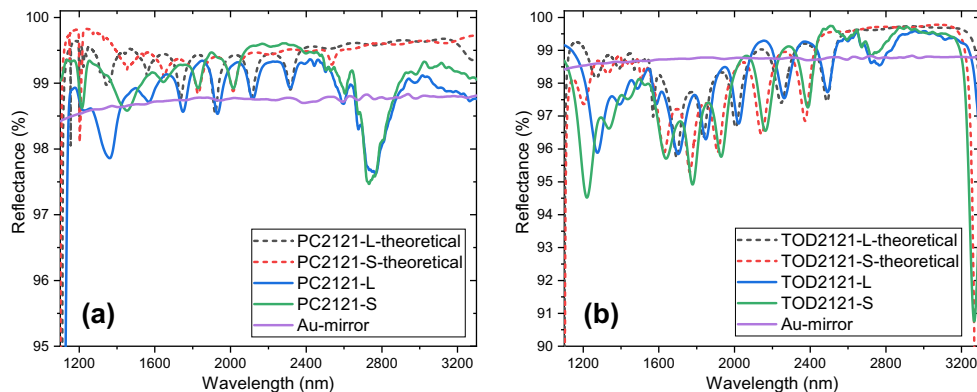


**Fig. 3.** (a) Reflectance of PC2121-L/S compared to the theoretical values. (b) Reflectance of TOD2121-L/S compared to the theoretical values.

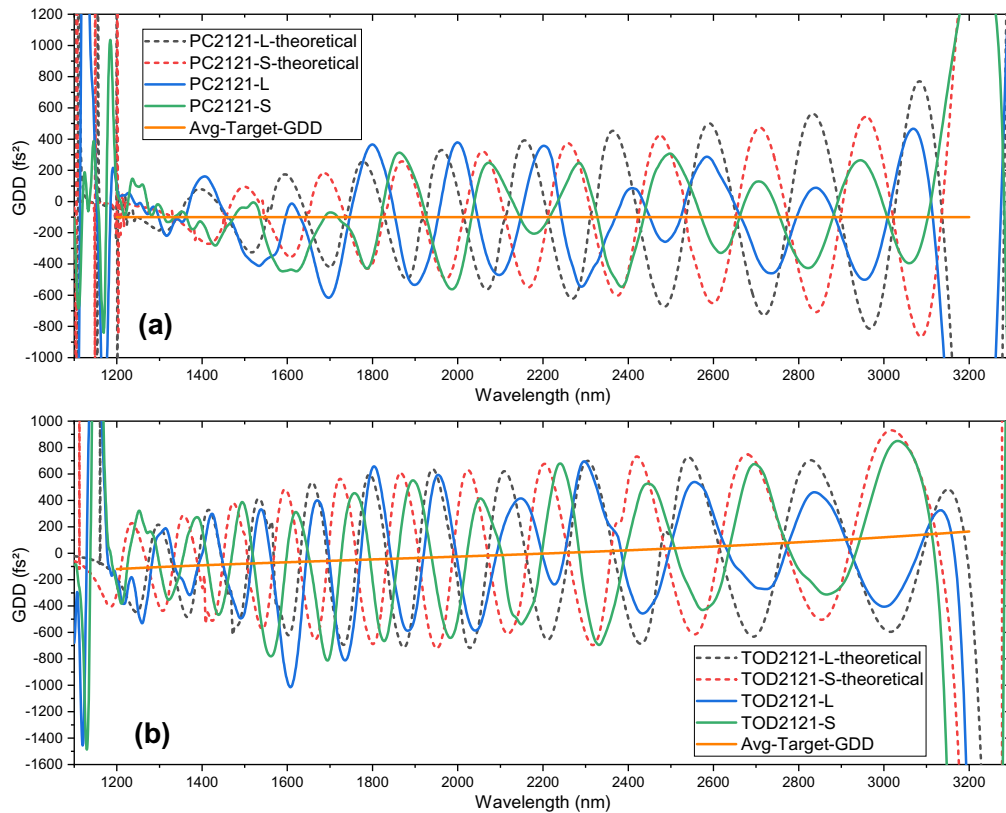


**Fig. 4.** Measured GDD of (a) PC2121-L/S and (b) TOD2121-L/S compared to the theoretical values and the average target GDD.

The GDD characteristics of the DMs were calculated from measurements with a self-built MIR white-light interferometer (WLI) [20]. It consists of the beforehand mentioned Vertex 70 FTIR spectrometer and a Michelson interferometer. Due to the high bandwidth ranging from the NIR to the MIR the measurements were split in two parts and later combined to one curve for each mirror. The spectral range from 1200-2500nm was measured with a standard tungsten-halogen light source, while the range from 2000-3200nm was measured with a silicon carbide globar MIR light source and a different beam splitter. The measurements overlap from 2000-2500nm which allows the combination of the results. In Fig. 4(a) the measured GDD of the mirror pair PC2121-L/S is presented in comparison to the theoretical values from Fig. 1(d). While the absolute values only match the theoretical ones in certain parts, a good agreement between theory and experiment can clearly be observed if the positions of the minima and maxima are compared. This shows that the two mirrors are matched to a high degree and will provide a significantly flattened GDD characteristic compared to a single mirror. Figure 4(b) then displays the measured GDD values of the TOD pair in comparison to the theoretical ones. A good agreement can be observed across the whole working range of the DM pair. For these four measurements the absolute results are also outstandingly close with only a few peaks being far away from the simulated values.

Finally, the impact of these mirrors on ultrashort laser pulses is presented. First, simulations were performed with the OptiLayer software. For this purpose an artificial Fourier transform limited super-gaussian laser pulse with a spectrum from 1200-3200nm and a full width of half maximum (FWHM) of 150THz was generated. The central wavelength was specified at 1900nm. Therefore, the input pulse has a pulse duration (PD) of 8.52fs. This pulse then accumulates the

in section 2 stated values for the reflectance target and the opposite GDD target. Due to the reflectance target being set to 100% there are no losses, but since the GDD target is set to  $-100\text{fs}^2$  for the PC2121-L/S, the pulse will degrade because of  $100\text{fs}^2$  of GDD that it picks up. The same holds for the TOD2121-L/S mirrors, only that the pulse will pick up the inverted GDD target from Fig. 2(d) instead. After that, the reflection from the mirrors is simulated. As a result of the imperfect reflectance and GDD characteristics of the DMs compared to the target values the pulse will not be recompressed completely and lose some intensity. Figure 5(a) shows the simulated results for the input pulse and the outcome after a different number of bounces from the two different mirror pairs. For PC2121-L/S the PD and intensity will basically not change even for a high number of bounces. Only for ten bounces from the pair, which means 20 reflections in total, 5% of the maximum intensity gets lost and the pulse is stretched slightly. For TOD2121-L/S on the other hand a faster degradation of the pulse quality can be observed due to the reduced reflectance and more complicated GDD characteristics. While the pulse is not stretched in time, nearly 5% of intensity are immediately lost upon reflection from the two individual DMs. For five bounces from the pair (ten total reflections) more than 35% of the intensity are lost and the pulse has been broadened to 9.6fs. Therefore, the TOD mirror pair should only be used once compared to the GDD pair which can be used several times without major losses.

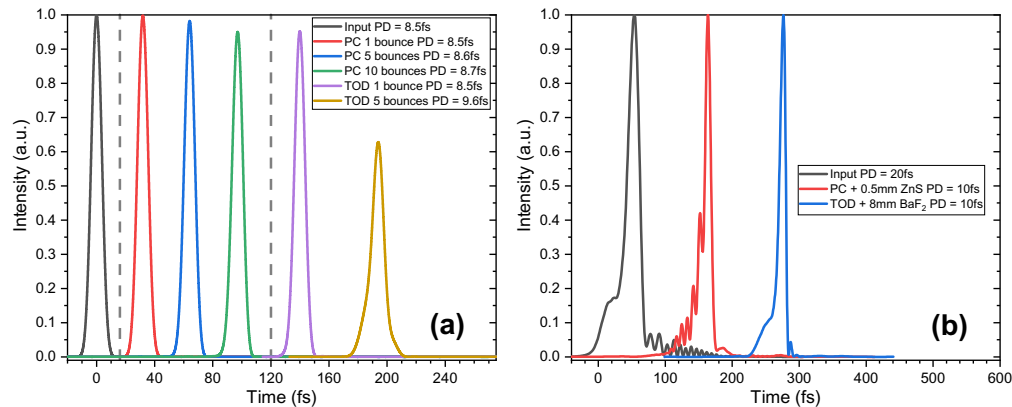


**Fig. 5.** (a) Simulated laser pulses after a varying number of bounces from the different mirror pairs. (b) Measured results of a Cr:ZnS laser system for different configurations.

For the measurements in Fig. 5(b) a home-built, all-reflective second-harmonic-generation frequency-resolved optical gating (SHG-FROG) instrument was used. The laser system generating the measured pulses is based on Cr:ZnS and provides a spectrum between  $1.2\text{-}3.2\mu\text{m}$ . The Fourier transform limited PD for this particular spectrum is around 7fs. The actual output from the laser is not compressed fully and has a PD of about 20fs (Fig. 5(b), black curve). Using the PC2121-L/S pair directly with this output completely overcompensates the GDD present in the pulse resulting in a PD of 26fs. Adding another pair makes it even worse giving a PD of 33fs. Therefore, a ZnS plate with a thickness of 0.5mm was placed in the beam to introduce some artificial GDD. The GDD of ZnS is positive in the whole working range of the mirrors. With this additional plate and a single pair of PC2121-L/S the pulse duration was shortened to 10fs (Fig. 5(b), red curve). Unfortunately ZnS also introduces a considerable amount of TOD which appears on the leading edge of the pulse. A substantially better beam profile was achieved with a pair of TOD2121-L/S and an additional 8mm of BaF<sub>2</sub> (Fig. 5(b), blue curve). BaF<sub>2</sub> has a positive GDD for wavelengths below  $2\mu\text{m}$  and a negative GDD for wavelengths above that. It is mainly used to compress the shorter wavelengths of the laser pulse in this setup. This configuration also resulted in a PD of 10fs but the obvious TOD was reduced drastically. This shows, that both

mirror pairs fulfill their design requirements and can provide significantly improved laser pulses compared to the initial input.

#### 4. Conclusion

Two different dispersive mirror pairs were successfully produced and carefully characterized. Additionally they were tested in a Cr:ZnS laser system showing their capability of dispersion control. The first mirror pair provides a nearly constant group delay dispersion of  $-100\text{fs}^2$  in the spectral range from 1.2-3.2 $\mu\text{m}$ . The second pair was tailored to compensate the third-order dispersion introduced by a 0.5mm thick TiO<sub>2</sub> crystal for the same spectral range. At the same time both mirror pairs maintain an unparalleled high reflectance. Covering a bandwidth of over 1.4 octaves is a significant progress over previously reported results for this wavelength range and will enable considerable improvements in laser systems like Cr:ZnS and others with a central wavelength around 2 $\mu\text{m}$ .

**Acknowledgments.** The authors thank Ferenc Krausz for many valuable discussions and his continued support for this work.

**Disclosures.** The authors declare no conflicts of interest.

**Data availability.** Data underlying the results presented in this paper are not publicly available at this time, but may be obtained from the authors upon reasonable request.

#### References

1. R. Szipöcs, K. Ferencz, C. Spielmann, and F. Krausz, "Chirped multilayer coatings for broadband dispersion control in femtosecond lasers," *Opt. Lett.* **19**(3), 201–203 (1994).
2. N. Matuschek, L. Gallmann, D. H. Sutter, G. Steinmeyer, and U. Keller, "Back-side-coated chirped mirrors with ultra-smooth broadband dispersion characteristics," *Appl. Phys. B* **71**(4), 509–522 (2000).
3. V. Pervak, F. Krausz, and A. Apolonski, "Dispersion control over the ultraviolet-visible-near-infrared spectral range with HfO<sub>2</sub>/SiO<sub>2</sub>-chirped dielectric multilayers," *Opt. Lett.* **32**(9), 1183–1185 (2007).
4. V. Pervak, M. K. Trubetskov, and A. V. Tikhonravov, "Robust synthesis of dispersive mirrors," *Opt. Express* **19**(3), 2371–2380 (2011).
5. V. Pervak, O. Razskazovskaya, I. B. Angelov, K. L. Vodopyanov, and M. Trubetskov, "Dispersive mirror technology for ultrafast lasers in the range 220–4500 nm," *Adv. Opt. Technol.* **3**(1), 55–63 (2014).
6. E. Fedulova, K. Fritsch, J. Brons, O. Pronin, T. Amotchkina, M. Trubetskov, F. Krausz, and V. Pervak, "Highly-dispersive mirrors reach new levels of dispersion," *Opt. Express* **23**(11), 13788–13793 (2015).
7. V. Pervak, T. Amotchkina, D. Hahner, S. Jung, Y. Pervak, M. Trubetskov, and F. Krausz, "Complementary Si/SiO<sub>2</sub> dispersive mirrors for 2–4  $\mu\text{m}$  spectral range," *Opt. Express* **27**(24), 34901–34906 (2019).
8. T. Amotchkina, M. Trubetskov, S. A. Hussain, D. Hahner, D. Gerz, M. Huber, W. Schweinberger, I. Pupeza, F. Krausz, and V. Pervak, "Broadband dispersive Ge/YbF<sub>3</sub> mirrors for mid-infrared spectral range," *Opt. Lett.* **44**(21), 5210–5213 (2019).
9. Y. Chen, D. Hahner, and V. Pervak, "3–6 $\mu\text{m}$  dispersive mirrors compensating for dispersion introduced by the GaAs crystal," *Appl. Opt.* **60**(29), 9249–9253 (2021).
10. N. Nagl, S. Gröbmeyer, V. Pervak, F. Krausz, O. Pronin, and K. F. Mak, "Directly diode-pumped, Kerr-lens mode-locked, few-cycle Cr:ZnSe oscillator," *Opt. Express* **27**(17), 24445–24454 (2019).
11. S. Vasilyev, I. Moskalev, V. Smolski, J. Peppers, M. Mirov, Y. Barnakov, V. Fedorov, D. Martyshkin, S. Mirov, and V. Gapontsev, "Kerr-lens mode-locked Cr:ZnS oscillator reaches the spectral span of an optical octave," *Opt. Express* **29**(2), 2458–2465 (2021).
12. A. Hemming, N. Simakov, J. Haub, and A. Carter, "High power resonantly pumped holmium-doped fibre sources," in *Optical Components and Materials XI*, vol. 8982 M. J. F. Digonnet and S. Jiang, eds., International Society for Optics and Photonics (SPIE, 2014), pp. 1–11.
13. P. Fuertjes, L. von Grafenstein, D. Ueberschaer, C. Mei, U. Griebner, and T. Elsaesser, "Compact OPCPA system seeded by a Cr:ZnS laser for generating tunable femtosecond pulses in the MWIR," *Opt. Lett.* **46**(7), 1704–1707 (2021).
14. Q. Wang, J. Zhang, A. Kessel, N. Nagl, V. Pervak, O. Pronin, and K. F. Mak, "Broadband mid-infrared coverage (2–17  $\mu\text{m}$ ) with few-cycle pulses via cascaded parametric processes," *Opt. Lett.* **44**(10), 2566–2569 (2019).
15. P. Steinleitner, N. Nagl, M. Kowalczyk, J. Zhang, V. Pervak, C. Hofer, A. Hudzikowski, J. Sotor, A. Weigel, F. Krausz, and K. F. Mak, "Single-cycle infrared waveform control," *Nature Photonics* (2022).
16. I. Pupeza, M. Huber, M. Trubetskov, W. Schweinberger, S. A. Hussain, C. Hofer, K. Fritsch, M. Poetzlberger, L. Vamos, E. Fill, T. Amotchkina, K. V. Kepesidis, A. Apolonski, N. Karpowicz, V. Pervak, O. Pronin, F. Fleischmann, A. Azzeer, M. Zigmán, and F. Krausz, "Field-resolved infrared spectroscopy of biological systems," *Nature* **577**(7788), 52–59 (2020).

17. A. V. Tikhonravov and M. K. Trubetskov, "OptiLayer software," <https://www.optilayer.com/>.
18. A. V. Tikhonravov, M. K. Trubetskov, and G. W. DeBell, "Optical coating design approaches based on the needle optimization technique," *Appl. Opt.* **46**(5), 704–710 (2007).
19. O. Humbach, H. Fabian, U. Grzesik, U. Haken, and W. Heitmann, "Analysis of OH absorption bands in synthetic silica," *J. Non-Cryst. Solids* **203**, 19–26 (1996). *Optical and Electrical Properties of Glasses*.
20. F. Habel, M. Trubetskov, and V. Pervak, "Group delay dispersion measurements in the mid-infrared spectral range of 2–20  $\mu\text{m}$ ," *Opt. Express* **24**(15), 16705–16710 (2016).